

Estimation of adipose compartment volumes in CT images of a mastectomy specimen

Abdullah-Al-Zubaer Imran^a, David D. Pokrajac^a, Andrew D.A. Maidment^b, Predrag R. Bakic^b

^aDepartment of Computer & Information Sciences, Delaware State University, Dover DE, 19901

^bDepartment of Radiology, University of Pennsylvania, Philadelphia, PA, 19104

ABSTRACT

Anthropomorphic software breast phantoms have been utilized for preclinical quantitative validation of breast imaging systems. Efficacy of the simulation-based validation depends on the realism of phantom images. Anatomical measurements of the breast tissue, such as the size and distribution of adipose compartments or the thickness of Cooper's ligaments, are essential for the realistic simulation of breast anatomy. Such measurements are, however, not readily available in the literature. In this study, we assessed the statistics of adipose compartments as visualized in CT images of a total mastectomy specimen. The specimen was preserved in formalin, and imaged using a standard body CT protocol and high X-ray dose. A human operator manually segmented adipose compartments in reconstructed CT images using ITK-SNAP software, and calculated the volume of each compartment. In addition, the time needed for the manual segmentation and the operator's confidence were recorded. The average volume, standard deviation, and the probability distribution of compartment volumes were estimated from 205 segmented adipose compartments. We also estimated the potential correlation between the segmentation time, operator's confidence, and compartment volume. The statistical tests indicated that the estimated compartment volumes do not follow the normal distribution. The compartment volumes are found to be correlated with the segmentation time; no significant correlation between the volume and the operator confidence. The performed study is limited by the mastectomy specimen position. The analysis of compartment volumes will better inform development of more realistic breast anatomy simulation.

Keywords: Anthropomorphic breast phantoms, anthropometry of adipose compartments, manual segmentation, mastectomy specimen, reconstructed CT image slices.

1. INTRODUCTION

The early detection has proven to be critical for the successful treatment of breast cancer, and in turn, for the reduction of related mortality. The early detection of breast cancer is achieved through the screening of asymptomatic women, based upon their age. Development of improved breast imaging systems is an ongoing research and industry effort. Validation of novel imaging systems has been conventionally performed via clinical imaging trials, which are long, costly and include the risk of repeated irradiation of volunteer women. Virtual clinical trials (VCTs) based upon the computer simulation of breast anatomy, imaging, and image analysis, represents a viable preclinical alternative. Our X-Ray Physics Lab at the University of Pennsylvania and MEDIS Lab at Delaware State University have extensive experience with the development of computer anthropomorphic breast phantoms¹⁻¹⁰ supporting VCTs of breast imaging systems. The breast anatomy shows a high variability in the spatial distribution of adipose and fibro-glandular tissues¹¹. In order to simulate this variability realistically, the simulation parameters (namely, the number, size, shape, and spatial distribution of adipose compartments, the thickness of Cooper's ligaments, etc.) must be selected from their realistic range of values. These ranges of values are not readily available in the anatomy literature; instead, they need to be estimated based upon the anatomical measurements from clinical data. The segmentation of clinical image data is the primary step for getting the adipose compartment volumes.

This work describes the estimation of the adipose compartment volumes by their segmentation from 3D reconstructed CT images of a mastectomy specimen. The volumes of the adipose tissue compartments have been determined as quantitative measure of their sizes; therefore, this two terms, size and volume, are used interchangeably. Because of the high resolution detail and clear visibility of the adipose tissue, CT scanned breast images have been chosen for this work.

The lack of homogeneity of the breast tissues and the subtle differences among neighboring tissues make it quite difficult to automatically segment CT images. Automatic CT image segmentation has been an ongoing research topics¹²⁻¹⁴. In order to determine values of simulation parameters for generating realistic breast phantoms, we have performed segmentation of adipose tissue compartments in 3D reconstructed CT images of a mastectomy specimen. After analyzing segmentation results, volumes of segmented adipose compartments have been estimated, and their distribution analyzed.

2. METHODS

2.1 Acquisition and Reconstruction of CT Image Slices

A total mastectomy specimen was donated to the University of Pennsylvania by an anonymous donor (after a gender reassignment surgery) and preserved in formalin. The specimen was imaged on a whole body, multi-slice CT system (Sensation 64, Siemens Medical Solutions USA, Malvern, PA), using the following acquisition parameters:

Acquisition Time: 72.318s	Station Name: CT54314
Study Description: Head^1_HEAD (Adult)	Body Part Examined: Chest
Slice Thickness: 0.6 mm	Tube Potential: 120 kVp
Tube Current: 400 mAs	Data Collection Diameter: 500 mm
Software Version: syngo CT_2006A	Protocol Name: 1_HEAD
Reconstruction Diameter: 500 mm	Exposure Time: 1000 ms
Focal Spot Size: 1.2mm	Distance Source to Detector: 1040 mm
Gantry/Detector Tilt: 0	Distance Source to Patient: 570 mm
ROI size: 371mm-by-371mm (512-by-512 array of 0.72mm-by-0.72mm pixels)	

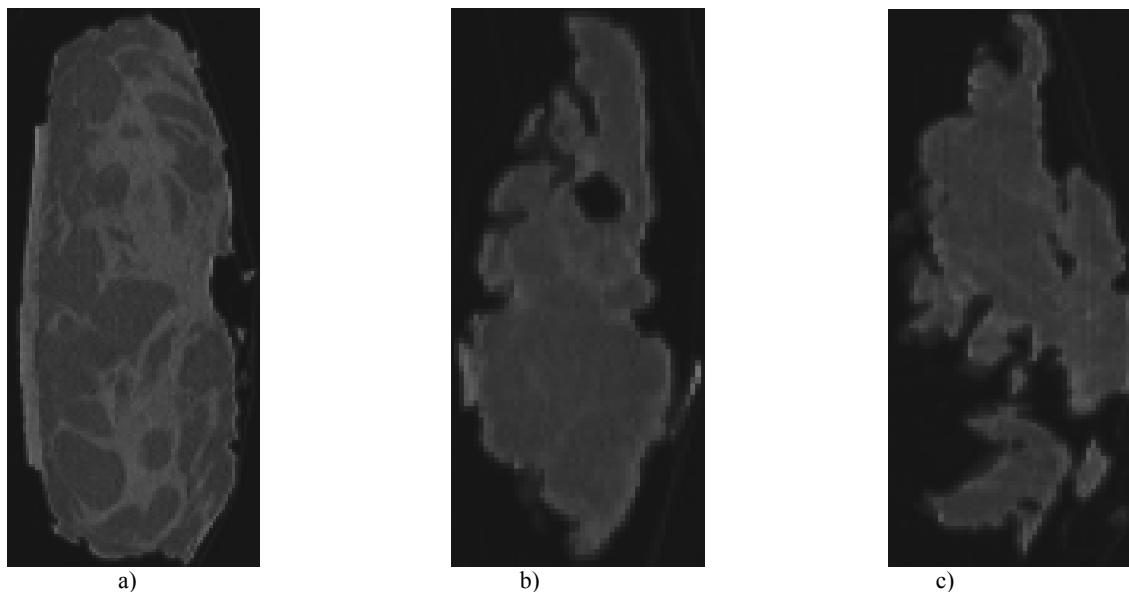


Figure 1. Examples of reconstructed CT images of the mastectomy specimen, used to estimate the volume of adipose compartments. Shown are (a) a reconstructed image with distinguishable adipose compartments; (b) an image with the contrast insufficient for a reliable identification of adipose compartments; and (c) an image with tissue regions separated by air due to discontinuities in the specimen. All images are shown after the contrast adjustment (described in Section 2.2.)

The image reconstruction resulted in 619 slices (each of 512*512 pixel size) saved in DICOM format. The slices 1-137 and 508-619 contained no tissue, only air; slices 138-160 and 467-507 had tissues without visible compartments; slices 161-466 contained breast tissues with visible adipose compartments. Therefore, among 619 CT slices we had 306 workable slices, where we could see the adipose compartments. Fig. 1 shows three sample slices where a sample slice with visibly distinguishable adipose tissue compartments, one with hardly visible compartments, and the other one disrupted with air within the tissue region.

2.2 Preprocessing and Contrast Adjustment

The reconstructed CT image slices were imported in open source ITK-SNAP software¹⁵ (version 3.2; <http://www.itksnap.org/pmwiki/pmwiki.php?n=Downloads.SNAP3>). A human operator was viewing the slices in the sequence, in order to get mental images of the position of compartments. All the CT image slices were zoomed assigning the common zoom factor value to 7.00px/mm for closer tissue view. To increase contrast, and make compartments easier to distinguish, we performed curve-based contrast adjustment. We moved the position of the image intensity vs. index into color map curve until we achieved a discernable view of the compartments. Fig. 2 shows the raw image slice along with contrast adjusted slices.

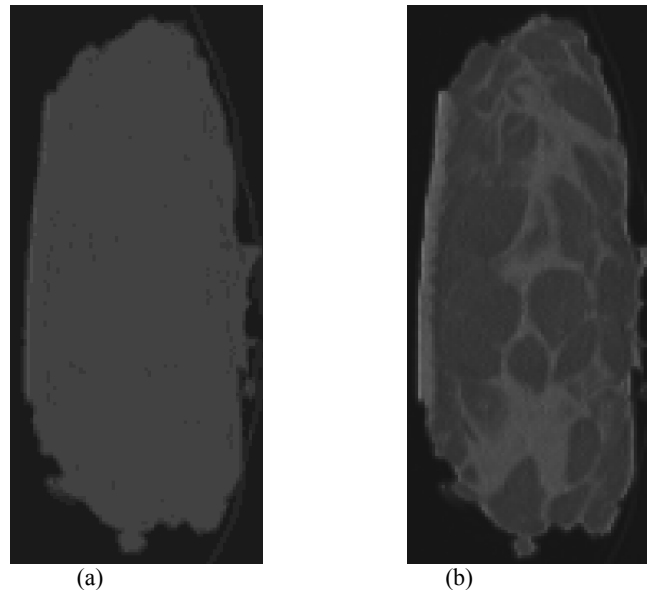


Figure 2. Image of one slice (403) of a CT image: a) unprocessed; b) contrast adjustment with manually adjusted parameters

2.3 Manual Segmentation

The main challenge in the process of manual segmentation was the fact that a compartment spans multiple slices, and that frequently several compartments occupy the same slice. Hence, it was decided that the human operator manually segments compartment by compartment. The segmentation started from compartments appearing the largest, which were easiest to observe. For each compartment, the operator determined the slices that a compartment occupied (by noting the first and the last slice). The operator chose a marking color in ITK-SNAP to distinguish the currently segmented compartments from the previously segmented. Then, for each slice containing the compartment, using Polygon Drawing Mode of ITK-SNAP tool, the operator marked a boundary of a compartment. To improve the quality of this work, this operation was performed in a room with dimmed light. Images were visualized on 23.6" LED monitor (DELL, 20*12.5).

Table 1. Levels of confidence and their qualitative description

Level of Confidence	Description
1	The compartment in the slice has invisible boundary. So, the boundary is marked by visual approximation of the operator.
2	The compartment in the slice has almost invisible boundary.
3	The compartment in the slice has hazy boundary.
4	The compartment in a slice has seemingly apparent boundary, still not exactly discernable.
5	The compartment in a slice has well distinguished boundary, so best possibly marked.

The operator indicated their level of confidence in segmenting a particular compartment from a slice (using numerical scale as shown in the Table 1). This was performed in order to pinpoint slice(s) where a compartment is not clearly visible (i.e., does not appear as clearly separated from the remaining tissue).

We segmented 205 most discernible adipose compartments from the 619 image slices. Fig. 3 shows the segmented adipose compartments in two different image slices, where relatively large numbers of segments exist (26 and 25). After the segmentation of all compartments was performed, using Segmentation Volume and Statistics option of ITK-SNAP tool, the number of voxels and volumes of each label for the segmented compartments were calculated. Fig. 4 shows the 3D representation of all 205 segmented adipose compartments as obtained from ITK-SNAP.

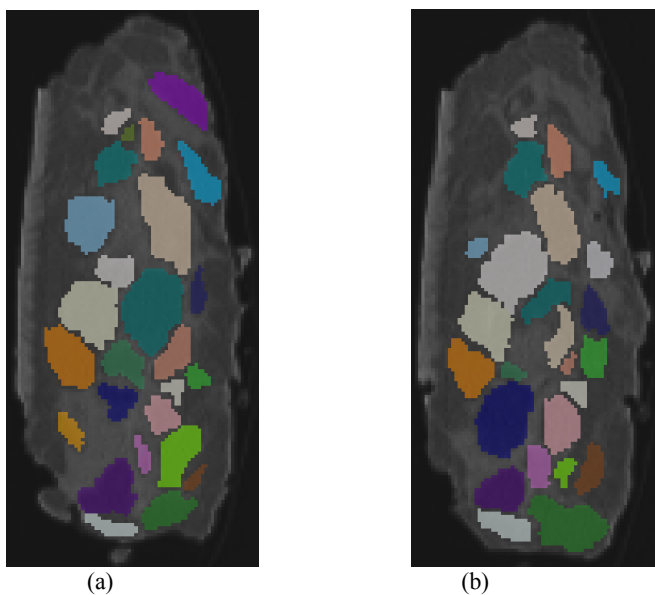


Figure 3. Adipose compartments in slices marked by manual segmentation. Fig. shows slices: (a) 385 and (b) 410

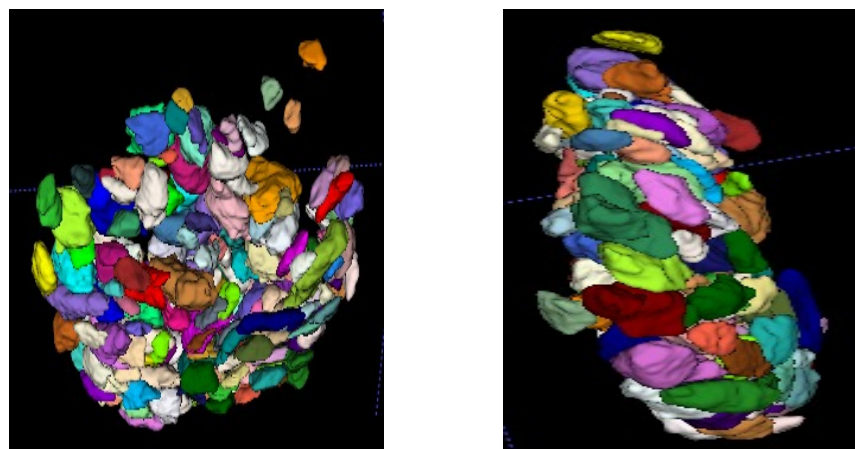


Figure 4. Two different views of the segmented 205 adipose compartments in ITK-SNAP

2.4 Statistical Testing and Analysis

Statistical analysis was performed on the estimated volumes, numbers of slices each compartment occupies and total time needed to segment adipose compartments. Our best interest was to check the distribution of estimated compartment volumes for the normality. As we know that any distribution being normal, would certainly make life easier. If we get the distribution of volume data as normal, then the statistical relationships associated with it would be very much

straightforward and tractable. The interpretation and assumption of adipose compartment volumes in real clinical images would be much easier then and so would be the extraction of simulation parameters associated with volumes. We therefore, performed quantile-quantile (QQ) plot¹⁶. In which, two sets of quantiles (from estimated volume data and theoretical normal data) were plotted against one another with scatterplot. If the data points roughly follow a straight line, then we can confirm the distribution of adipose compartment volume is normal. Then, the Kolmogorov-Smirnov test (KS-test)¹⁷ was performed to check for the normality of compartment volumes distribution. For the confirmation of the result achieved from KS-test, we also performed the Lilliefors test¹⁸ and Jarque-Bera test¹⁹. To be noted that, the null hypothesis (the distribution of estimated volumes is normal) was tested at 5% significance level. The statistical correlations among the compartmental volume, segmentation time, and average confidence level were also determined and analyzed.

3. RESULTS AND DISCUSSION

3.1 Adipose Compartment Volume and Segmentation Time

The segmentation resulted associated with the time taken in each slice for segmenting 205 adipose compartments. The average time for segmenting a compartment is 8.75 minutes and a compartment spans on average 20 reconstructed CT slices. Fig. 5 shows the histogram of number of slices belonging to the segmented adipose compartments. We can see that most of the segmented adipose compartments span between 10-20 slices and just a few compartments spanned more than 40 slices.

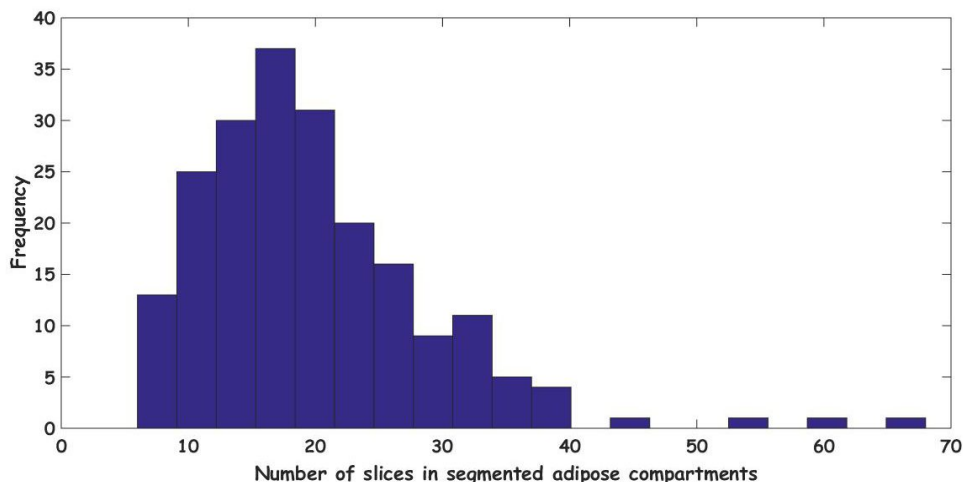


Figure 5. Histogram of number of slices spanned by segmented compartments

Fig. 6 contains histogram of estimated compartmental volumes. Based on results, the average estimated compartmental volume is 0.91 cm³ (standard deviation 0.87 cm³). Note that this average value is very close to the estimated subcutaneous compartmental volumes reported from histological image data⁸, although standard deviation is much higher. One of the reasons for this high variance might, however, be selection bias (the operator first processed compartments of varying sizes which are more clearly visible). Again, a probable reason is the fact that the small path sample includes a limited tissue area, with potentially limited variation in the compartment size.

The scatter plot of segmentation time vs. compartment volume has been shown in Fig. 7. The Pearson's correlation indicates that the segmentation time for a compartment is correlated with its volume (p-value ≈ 0). The results suggest that the standard deviation of residuals may increase with the estimated volume size, indicating the heteroscedasticity.

3.2 Distribution of Estimated Compartment Size

We examined the normality of the estimated compartment sizes using the quantile-quantile plot and statistical tests. The quantile-quantile (QQ) plot in Fig.8 indicates that the distribution of estimated adipose compartment volumes is not normal. As we can see from the QQ plot, the blue filled circles corresponding to the quantiles of the observed

distribution starting from the left of the normal line and, after crossing it, move to the other side again. This behavior confirms the skewness that can be observed from histogram in Fig. 6 (the histogram is left-skewed).

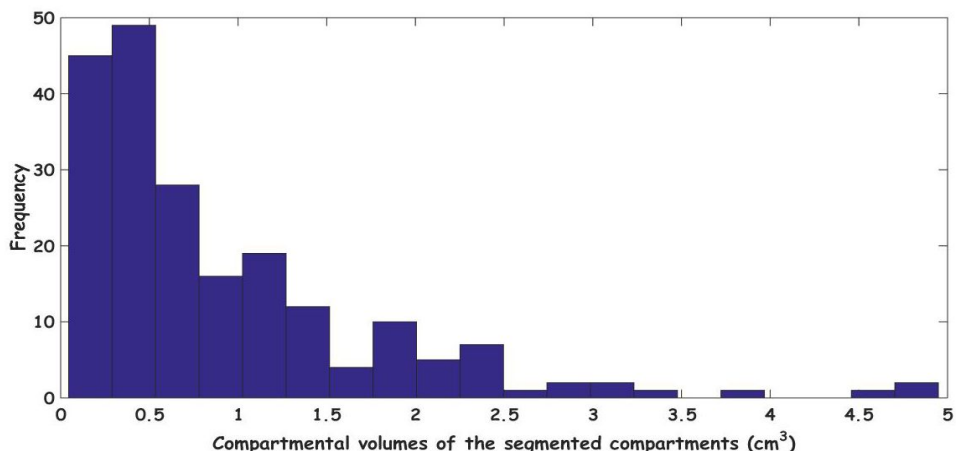


Figure 6. Histogram of estimated compartmental volumes

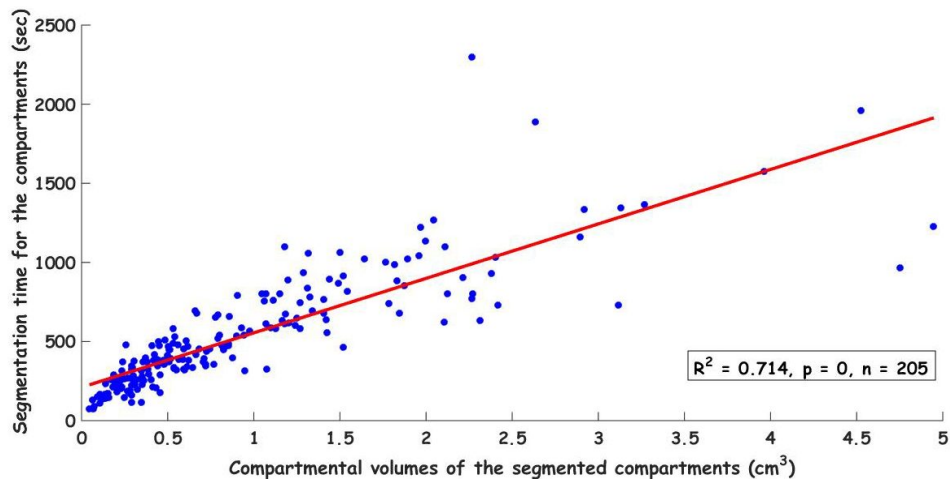


Figure 7. Segmentation time Vs compartmental volumes for 205 segmented compartments.

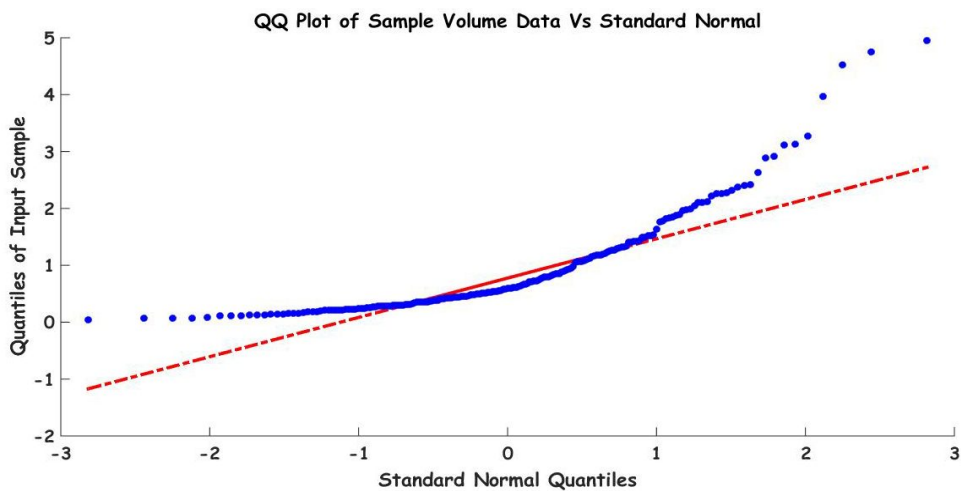


Figure 8. QQ Plot of Sample Volume Data Vs Standard Normal

The Kolmogorov-Smirnov test (KS-test) was performed to check for the normality of compartment volumes distribution. The test rejected the normality hypothesis with $p\text{-value} < 0.0001$. This result was confirmed with the Lilliefors test and Jarque-Bera test ($p\text{-value} < 0.001$). The visual comparison of the empirical cumulative distribution function (cdf) and the standard normal cdf is shown in Fig. 9. The compartment volume data were standardized (to have zero mean and unit standard deviation).

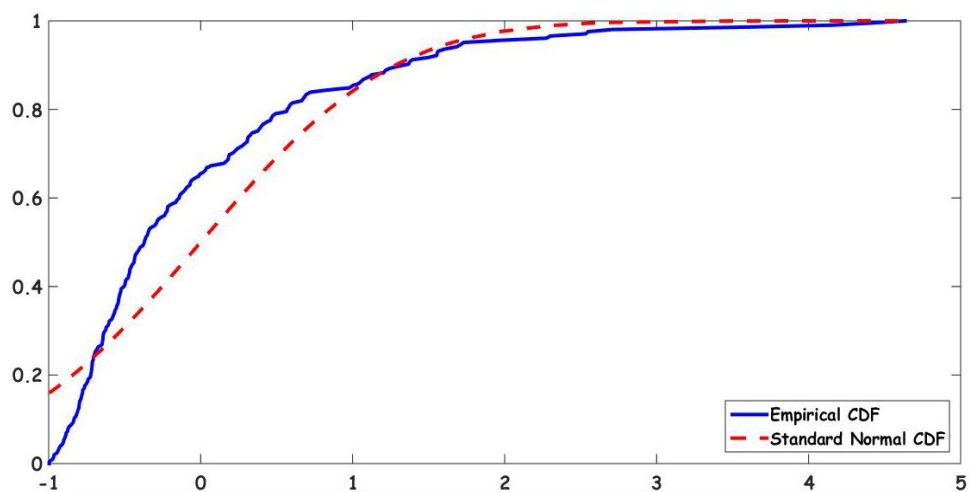


Figure 9. Empirical cdf of the centered and scaled Volume and the cdf of the standard normal distribution

3.3 Volumes of Segmented Compartments vs. Segmentation Confidence

Fig. 10 shows the histogram of the average confidence level in segmenting adipose compartments from CT slices. The confidence level was assigned in the scale of 5 while segmenting every slice, as explained in Section 2.3. The average confidence in 205 segmented compartments was 3.88. As we can see in the Fig. 11, the large compartments are segmented with lower confidence than the medium sized compartments. Again, the smaller-sized adipose compartments had confidence levels in the whole range.

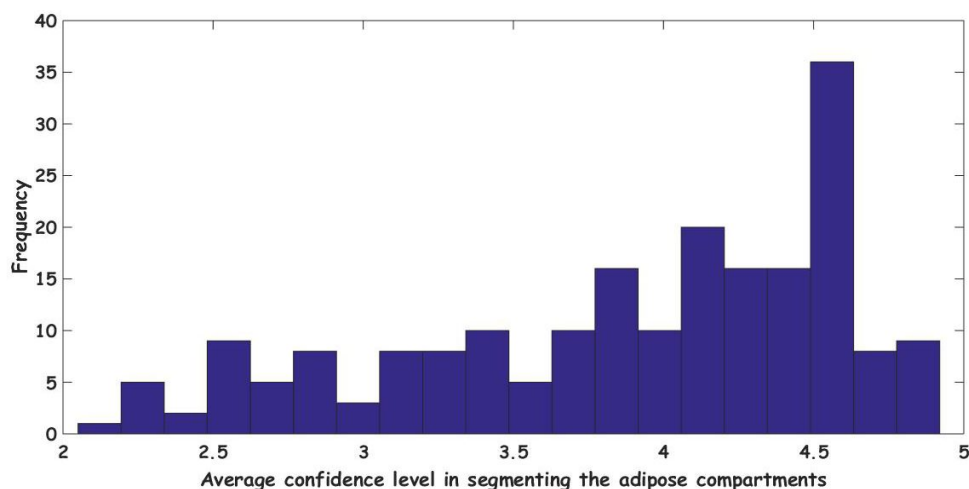


Figure 10. Histogram of Average Confidence Level in Segmenting Compartments

3.4 Significance of the Outcome

The manual segmentation with boundary marking of the adipose compartments was undertaken without readily available a feasible automated technique. We have shown the estimation of adipose compartment volumes based on this

segmentation. The segmentation result demonstrated that the total segmentation time is dependent on the estimated size of each adipose compartment. On the other hand, the compartment size is not correlated with the average confidence level of segmentation. The possible reason is confidence level was assigned by the operator based on subjective visibility of the compartment rather than the size. The distribution of the estimated volumes is not normal and is left-skewed. The skewness of the distribution might however be a consequence of a selection bias, where an operator did not select large, but well-discernable compartments. An automated segmentation method would be utilized for the repetition of the volume estimation. The comparison of the resultant volumes from manual and future automatic segmentation will provide more decisive extraction of realistic simulation parameters. The shape analysis of simulated adipose tissue compartments provided the assessment of relationship between input simulation parameters and final appearance of breast phantoms²⁰. The extraction of shapes, sizes, and orientations of adipose compartments would be performed for the estimated volumes based on clinical imaging, following the approach in the spatial distribution²¹.

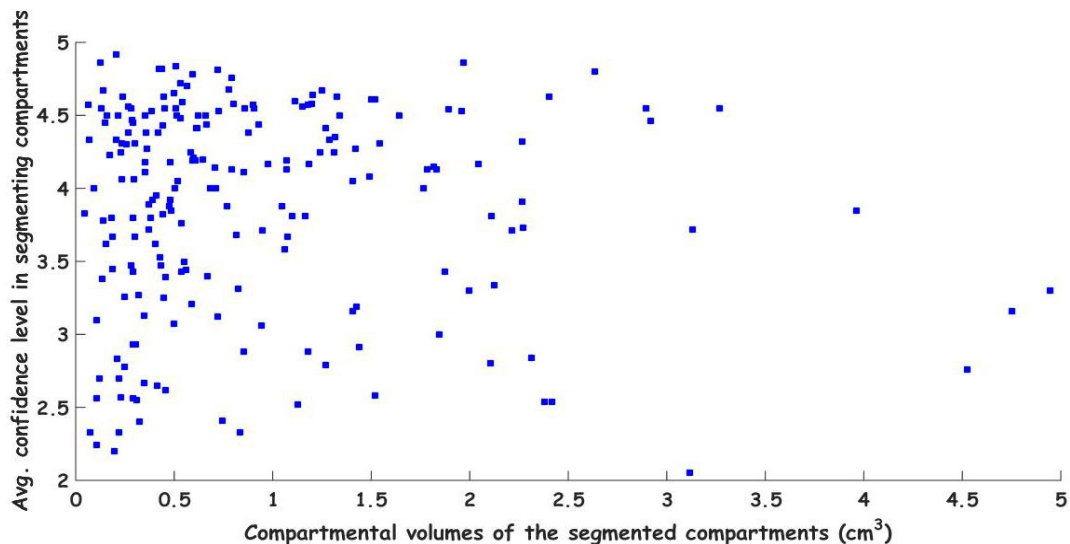


Figure 11. Confidence in manual segmentation Vs compartmental volume

4. CONCLUSIONS

This work has been performed as an initial step for our goal of improving realism in the development of anthropomorphic software breast phantoms. We have presented a proof of concept that realistic descriptors of the breast internal anatomical structures (namely, the size of the adipose tissue compartments) could be estimated through manual segmentation of clinical images. In our study, we used reconstructed high-dose CT images of a normal mastectomy specimen. The future work would be aimed at developing an automatic segmentation in order to achieve faster and unbiased segmentation. The limitation of this work is that the mastectomy specimen used in reconstruction CT slices differs from “in-vivo” breast. It was detached from the body and was preserved into formalin. The internal tissue structures were most likely deformed. Hence, it is of interest to perform estimation of adipose compartments volume based on CT or MRI breast clinical images. Moreover, the volume estimation would provide the associated parameters extraction for the breast imaging simulation. The informed selection of realistic simulation parameters would improve the user control in generating anthropomorphic software breast phantoms.

ACKNOWLEDGEMENTS

This research was supported by a grant from the National Institute of General Medical Sciences (P20 GM103446) from the National Institutes of Health. Also, the work was supported in part by the US Department of Defense Breast Cancer Research Program (HBCU Partnership Training Award #BC083639), the US National Science Foundation (CREST grant #HRD-1242067), the US Department of Defense/Department of Army (Award #W911NF-11-2-0046), the US National Institutes of Health (R01 grant #CA154444), and the Komen Foundation (grant #IIR13262248). The content is solely the responsibility of the authors and does not necessarily represent the official views of the NIH, DoD, and Komen

Foundation. The authors are thankful to Mr. Scott Cupp from the University of Pennsylvania for his assistance with the CT image acquisition.

REFERENCES

- [1] Bakic, P.R. and Brzakovic, D., "Simulation of digital mammogram acquisition," Proc. SPIE 3659, 866-877 (1999).
- [2] Bakic, P. R., Brzakovic, D. and Zhu, Z., "Anatomic segmentation of mammograms via breast model," Proc. IWDM 4, 291-294 (1998).
- [3] Bakic, P. R., Brzakovic, D., Brzakovic, P. and Zhu, Z., "An approach to using a generalized breast model to segment digital mammograms," Proc. IEEE CMBS 11, 84-89 (1998).
- [4] Bakic, P. R., Albert, M., Brzakovic, D. and Maidment, A. D. A., "Mammogram synthesis using a 3D simulation. I. Breast tissue model and image acquisition simulation," Med. Phys. 29(9), 2131-2139 (2002).
- [5] Bakic, P. R., Albert, M., Brzakovic, D. and Maidment, A. D. A., "Mammogram synthesis using a 3D simulation. II. Evaluation of synthetic mammogram texture," Med. Phys. 29(9), 2140-2151 (2002).
- [6] Bakic, P. R., Albert, M., Brzakovic, D. and Maidment, A. D. A., "Mammogram synthesis using a three-dimensional simulation. III. Modeling and evaluation of the breast ductal network," Med. Phys. 30(7), 1914-1925 (2003).
- [7] Zhang, C., Bakic, P. R. and Maidment, A. D. A., "Development of an anthropomorphic breast software phantom based on region growing algorithm," Proc. SPIE 6918, 69180V (2008).
- [8] Bakic, P. R., Pokrajac, D. D., Caro, R. D. and Maidment, A. D. A., "Realistic simulation of breast tissue microstructure in software anthropomorphic phantoms," Proc. IWDM 8539, 348-355 (2014).
- [9] Pokrajac, D. D., Maidment, A. D. A. and Bakic, P. R., "A method for fast generation of high resolution software breast phantoms," Med. Phys. 38(6), 3431 (2011).
- [10] Pokrajac, D. D., Maidment, A. D. A. and Bakic, P. R., "Optimized generation of high resolution breast anthropomorphic software phantoms," Med. Phys. 39(4), 2290-2302 (2012).
- [11] Geddes, D. T., "Inside the lactating breast: The latest anatomy research," Midwifery Womens Health. 52(6), 556-63 (2007).
- [12] Kuo, H.-C., Giger, M. L., Reiser, I., Boone, J. M., Lindfors, K. K., Yang, K., and Edwards, A., "Level set segmentation of breast masses in contrast-enhanced dedicated breast CT and evaluation of stopping criteria," Digital Imaging. 27(2), 237-247 (2014).
- [13] Kuo, H. -C., Giger, M. L., Reiser, I., Drukker, K., Boone, J. M., Lindfors, K. K., Yang, K., Edwards, A. and Sennett. C. A., "Segmentation of breast masses on dedicated breast computed tomography and three-dimensional breast ultrasound images," Med. Imag. 1(1), 014501 (2014).
- [14] O'Connor, J. M., Das, M., Dider, C. S., Mahd, M. and Glicka, S. J., "Generation of voxelized breast phantoms from surgical mastectomy specimens," Med. Phys. 40(4), 041915 (2013).
- [15] Yushkevich, P. A., Piven, J., Hazlett, H. C., Smith, R. G., Ho, S., Gee, J.C., and Gerig, G., "User-guided 3D active contour segmentation of anatomical structures: Significantly improved efficiency and reliability," Neuroimage 31(3), 1116-28 (2006).
- [16] Wilk, M. B. and Gnanadesikan, R., "Probability plotting methods for the analysis of data," Biometrika 55(1), 1-17 (1968).
- [17] Massey, F. J., "The Kolmogorov-Smirnov test for goodness of fit," American Statistical Association 46(253), 68-78 (1951).
- [18] Lilliefors, H., "On the Kolmogorov-Smirnov test for normality with mean and variance unknown," American Statistical Association. 62, 399-402 (1967).
- [19] Jarque, C. M., and Bera, A. K., "A Test for normality of observations and regression residuals," Int. Statistical Review 55(2), 163-172 (1987).
- [20] Contijoch, F., Lynch, J.M., Pokrajac, D. D., Maidment, A. D. A. and Bakic, P. R., "Shape analysis of simulated breast anatomical structures," Proc. SPIE 8313, 83134J (2012).
- [21] Imran, A. -A. -Z., Bakic, P. R. and Pokrajac, D. D., "Spatial distribution of adipose compartments size, shape and orientation in a CT breast image of a mastectomy specimen," IEEE SPMB Symposium Dec. 13 (2015).